

Spring 2018

The Mechanism of Biotremor Production in the Veiled Chameleon (*Chamaeleo calyptratus*)

Samuel Tegge

Western Kentucky University, samuel.tegge087@topper.wku.edu

Follow this and additional works at: <https://digitalcommons.wku.edu/theses>



Part of the [Evolution Commons](#), [Integrative Biology Commons](#), and the [Systems and Integrative Physiology Commons](#)

Recommended Citation

Tegge, Samuel, "The Mechanism of Biotremor Production in the Veiled Chameleon (*Chamaeleo calyptratus*)" (2018). *Masters Theses & Specialist Projects*. Paper 2336.
<https://digitalcommons.wku.edu/theses/2336>

This Thesis is brought to you for free and open access by TopSCHOLAR®. It has been accepted for inclusion in Masters Theses & Specialist Projects by an authorized administrator of TopSCHOLAR®. For more information, please contact topscholar@wku.edu.

THE MECHANISM OF BIOTREMOR PRODUCTION IN THE VEILED CHAMELEON
(*CHAMAELEO CALYPTRATUS*)

A Thesis
Presented to
The Faculty of the Department of Biology
Western Kentucky University
Bowling Green, Kentucky

In Partial Fulfillment
Of the Requirements for the Degree
Master of Science

By
Samuel M. Tegge

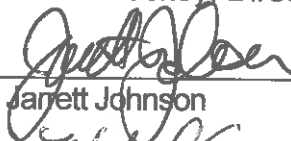
May 2018

THE MECHANISM OF BIOTREMOR PRODUCTION IN THE VEILED CHAMELEON
(CHAMAELEO CALYPTRATUS)

Date Recommended 7/10/18



Dr. Steve Huskey, Director of Thesis



Dr. Janett Johnson



Dr. Michael Smith



Dean, Graduate School

4/20/18

Date

I dedicate this thesis to my fiancé, Lindsey, my family, and my friends. Your constant friendship, love, and support have led me to this point. Thank you.

First and foremost, I would like to thank Dr. Steve Huskey for his guidance and support throughout this process, and for teaching me to appreciate the beauty that is inherent in the seemingly infinite variations of the vertebrate skeleton. I also want to thank Dr. Jarrett Johnson for his guidance while navigating the sometimes-treacherous world of statistical analyses. I now have a new-found love for data, statistics, and the stories that they can tell. And, without the expertise, mentorship, and hospitality of Dr. Chris Anderson, these data would not have been collected and this story not told. No good story is told without equally good visuals, so I must thank Dr. John Andersland, expert photographer and microscopist, for teaching me how to use the syncroscopy microscope. Lastly, I would like to thank Dr. Michael Smith for his pointed comments and critiques that guided me through the editing process.

Table of Contents

1	INTRODUCTION	1
	1.1 ANIMAL COMMUNICATION	1
	1.2 CHAMELEONS.....	4
	1.3 BIOTREMOR PRODUCTION.....	6
2	MATERIALS AND METHODS	8
	2.1 CHAMELEON HOUSING AND CARE	8
	2.2 ELECTRODE CONSTRUCTION.....	8
	2.3 SURGERY	8
	2.4 EMG AND ACCELEROMETRY	9
	2.5 STATISTICAL ANALYSIS	10
3	RESULTS	13
	3.1 CORRELATION OF MUSCULAR ELECTRICAL ACTIVITY AND BIOTREMOR ACTIVITY.....	13
	3.2 MECHANISTIC DESCRIPTION	13
	3.3 SEXUAL DIMORPHISM	15
4.	DISCUSSION	16
	4.1 CORRELATION OF BIOTREMOR AND MUSCLES	16
	4.2 MECHANISTIC DESCRIPTION	17
	4.3 SEXUAL DIMORPHISM	19
5	CONCLUSION	21
6.	REFERENCES	22
7.	TABLES	26
8.	FIGURES	35

THE MECHANISM OF BIOTREMOR PRODUCTION IN THE VEILED CHAMELEON
(*CHAMAELEO CALYPTRATUS*)

Samuel M. Tegge

May 2018

54 pages

Directed by: Dr. Steve Huskey, Dr. Michael Smith, and Dr. Jarrett Johnson

Department of Biology

Western Kentucky University

Vibratory communication has evolved in numerous animal groups, including insects, spiders, fishes, mammals, and was recently discovered in veiled chameleons (*Chamaeleo calyptratus*). I examined the mechanism by which *C. calyptratus* produce these biotremors. Muscle activity data were gathered during simulated anti-predator responses via electromyography (EMG) with simultaneous recordings of biotremor production using an accelerometer. I correlated EMG data with the accelerometer data to implicate the muscles responsible for the production of the biotremors. Mixed-effect linear regression models described the mechanism, and a model selection framework determined which model fit the data best. I then used an analysis of variance to partition the variance to each variable to determine which muscles were most important in the biotremor producing mechanism. The *Mm. sternohyoideus superficialis et profundus*, *Mm. mandibulohyoideus*, and *M. levator scapulae* were active during the production of biotremors. Mean latency calculations revealed that the *M. levator scapulae* and *Mm. mandibulohyoideus* activated prior to the vibration onset, and the *Mm. sternohyoideus superficialis et profundus* activated after the vibration onset. The *M. sternohyoideus superficialis* then ceased activity prior to vibration cessation, and the *M. sternohyoideus profundus*, *Mm.*

mandibulohyoideus, and *M. levator scapulae* ceased activity after the vibration had ended. The description of the biotremor producing mechanism further supports that *C. calyptratus* can produce biotremors, possibly for communication.

1 Introduction

1.1 Animal Communication

Animal communication is essential to the fitness of individuals, the success of populations, and the evolution of species (Endler 1993; Bass & Clark 2003; Bradburry and Vehrencamp 2011; Searcy and Nowicki 2012).

Communication mechanisms are shaped by the selective pressures of ecological niches, which include all biotic (intra- and interspecific interactions) and abiotic factors (*e.g.*, temperature, transmission medium, geometry of reflective surfaces, and composition of boundaries) (Endler 1993; Bass & Clark 2003; Searcy and Nowicki 2012). The myriad mechanisms observed in nature are a result of these selective pressures. For example, vibratory communication of insects emerged from living on dense plant matter, which is highly conducive to the transduction of vibrations, for millions of years (Hill & Wessel 2016). Complex acoustic vocalizations of passerine birds developed for communication through the air and through densely populated forests and grasslands (Beckers 2011). Seismic communication allows elephants to communicate over long distances across the African savanna (O'Connell-Rodwell *et al.* 2001, O'Connell-Rodwell 2007).

Vertebrate mechanisms of communication have specifically evolved for effective transmission of signals through Earth's crust, water, plant substrate, and air (Endler 1993). Most mammals and some lizards employ the vibration of vocal cords, which is housed in the larynx, to produce a limited number of vocalizations (Raghavendra *et al.* 1987); whereas most birds utilize the syrinx, which can

produce a larger repertoire of songs (Fee *et al.* 1998; Smyth & Smith 2002; Elemans *et al.* 2003). Some fishes produce acoustic signals via muscles that vibrate the swim bladder (Fine *et al.* 2001), while others use pectoral spines to drum the swim bladder to produce sound (Fine *et al.* 1997). Certain species of herring also communicate via explosive expulsions of air from their anuses (Wilson *et al.* 2004). Many reptiles and amphibians lack vocal folds or a syrinx and are considered “silent.” However, frogs use arytenoid cartilage ridges of the trachea to modulate sound production (Given 1987), and some lizards have been documented hissing (Moore *et al.* 1991; Labra *et al.* 2007). Many of these strategies are well studied, but much remains to be understood about true vertebrate vibratory communication.

True vibratory communication is defined by the use of biotremors to deliberately send information to an intended receiver to the benefit of both parties. Biotremors are vibrational signals that are transmitted through a solid substrate (*e.g.*, plant matter, soil, etc.). Biotremors are produced as Rayleigh surface waves, which are a type of seismic surface wave that occur at a boundary between two distinct media where particles are oscillated both perpendicular and parallel to direction of the wave’s propagation (Hill & Wessel 2016). Biotremors can be produced by the stridulation of an insect’s wing or the contraction of muscles, much like an acoustic signal is generated. However, the distinction between an acoustic signal and a biotremor is the medium through which the signal is transmitted, acoustic signals travel through the air and biotremors through a substrate. The only notable examples of true vibratory

communication are found in elephants, insects, and blind-subterranean mole rats (Heth *et al.* 1987; O'connell-Rodwell 2007; Hill & Wessel 2016). For example, elephants contract their laryngeal muscles to produce biotremors that travel through the ground and are received by fatty tissues on the bottom of the foot pads of other elephants (O'connell-Rodwell *et al.* 2001; O'connell-Rodwell 2007). There is also evidence from museum specimens that suggests some extinct amphibians were capable of vibratory communication, but may have only been capable of detecting vibrational signals not producing them (Hildebrand & Goslow 1985).

The detection of vibrational signals from prey or predators (Hildebrand & Goslow 1985) and the production of biotremors as a defense mechanism do not constitute true communication because the information conveyed by these biotremors does not explicitly benefit the sender and receiver. These defense signals are often produced by prey species, and they are created with the same muscles or organs that are used to generate the signals for true communication. For example, many mammals, including primates and sciurid rodents, also produce defense signals using the same mechanism that is used in true communication (Macedonia & Evans 1993).

Barnett *et al.* (1999) documented the use of biotremors (50-150 Hz), accompanied with an audible hoot, by *Chamaeleo calypttratus* during courtship, copulation, and territorial displays. *C. calypttratus* and ground-dwelling chameleons have also been documented producing biotremors as a defense mechanism (Barnett *et al.* 1999; Tolley & Herrel 2014). Ground-chameleons use

biotremors to shake off smaller insects (e.g., ants) that may prey on them, while also remaining in a cryptic state (Tolley & Herrel 2014). The ability to generate biotremors adds to the growing list of chameleon peculiarities.

1.2 Chameleons

Chameleons evolved in East Africa, and later colonized the Ethiopian, Palearctic, and Oriental geographic regions (Tolley & Herrel 2014). Currently, chameleons inhabit Africa (including Madagascar and the Seychelles), Southern Europe, the Southern Arabian Peninsula, and the Near East. A small number of species have also been introduced to Hawaii, California, and Florida (Tolley & Herrel 2014). Chameleons live in a wide range of environments within these geographical regions: the tropical rainforests of Madagascar, alpine grasslands of the Ugandan Ruwenzori Mountains, Ruwenzori Mountain forests of Ethiopia, savannahs and shrubby habitats, deserts, and semi-deserts (Tolley & Herrel 2014).

Chameleons have evolved many specialized characteristics, such as prehensile tails and fused, opposing digits for maneuvering in arboreal environments, turreted and independently moving eyes with negatively powered lenses for accommodation, ballistic tongues, chemically modulated prey-luring, and rapid physiological color change behaviors that all help make chameleons voracious predators (Measy *et al.* 2009; Huskey 2017). Many also possess a water-catching casque that collects water and funnels it to the mouth (Measy *et al.* 2009; Huskey 2017). Extreme sexual dimorphism is also observed in many

species. For example, in *C. calyptratus*, males are larger (mass, snout-vent length, etc.), have larger casques, possess spurs on their hind limbs, and possess a larger repertoire of colors (Tolley & Herrel 2014). Chameleon's unique characteristics have made the most studied squamate (Tolley & Herrel 2014). However, research has yet to elucidate the many complexities of their behavior. For example, it has long been thought that chameleons only communicate via physiological changes in color, but, as previously mentioned, there is evidence that *C. calyptratus* use biotremors (Barnett *et al.* 1999) for intraspecific communication (*i.e.*, courtship, territoriality, and mating) and interspecific communication (*i.e.*, defense mechanism or distress signal). However, according to Tornier (1905) and further supported by Huskey (unpublished data), chameleons lack a syrinx and true functional vocal cords that are thought to be needed to facilitate biotremor production accompanied by a vocalization (audible hoots). Wever (1968, 1969a, 1969b) demonstrated that chameleons have reduced hearing due to the lack of an external ear (pinna) and tympanic membrane. However, Hartline (1971) has compared the auditory structures of chameleons to that of snakes and found that the structures are theoretically capable of detecting biotremors. The absence of a syrinx, vocal cords, and external ears (Wever 1968; Wever 1969a; Wever 1969b; Measey *et al.* 2009) paired with the theoretical ability to detect biotremors (Hartline 1971; Barnett *et al.* 1999) suggest an alternative mechanism of communication among *C. calyptratus*.

1.3 Biotremor Production

Approximately 20 of the 200 species of chameleons (Glaw 2015) possess a gular pouch (Figure 1), an out-pocketing of the trachea housed ventrally and posteriorly to the lower jaw and superiorly to the hyoid retractor muscles (Huskey pers. obs.; Tornier 1905; Germershausen 1913). The gular pouch of each species has a unique morphology (Figure 2; Tornier 1905; Germershausen 1913), but its function has yet to be determined. I examined activity of the *Mm. mandibulohyoideus*, *M. sternohyoideus superficialis*, and *M. sternohyoideus profundus* because of their close association with the gular pouch (Figure 3). I chose the *Mm. levator scapulae* due to observations by Barnett *et al.* (1999) that a head-click (a rapid side-to-side movement of the head) is observed with biotremors. I used the *Mm. triceps* as a control muscle. *C. calyptratus* produce biotremors as a defense mechanism, which provides a reliable and repeatable framework with which to elicit a biotremor from a chameleon.

I hypothesized that the hyoid retractor muscles produce the biotremor, and the gular pouch acts as an amplifier of the biotremor to produce the audible hoot that was observed by Barnett *et al.* (1999). The biotremor producing mechanism is similar to the specialized sonic muscles surrounding the swim bladder of some fishes. It is theoretically possible to create a biotremor without the gular pouch (*i.e.*, the defensive biotremors observed in *C. calyptratus* and ground-dwelling chameleons). However, the gular pouch may be necessary for the production of the audible hoot associated with the true communication observed by Barnett *et al.* (1999), but not necessary for the production of the biotremor itself. It is then

conceivable that the muscles responsible for producing biotremors in an antipredator context are the same that produce biotremors as a means of true communication.

I used *C. calyptratus* because Barnett *et al.* (1999) demonstrated that biotremors are easily elicited from this species. I employed electromyography (EMG) and accelerometry to (1) correlate the electrical activity of the muscles with the biotremor, (2) determine the order of muscle activity during biotremor production, (3) establish the muscles responsible for biotremors, (4) elucidate which muscles play an important role in the duration of the biotremors, and (5) illuminate any sexual dimorphism present in the biotremor frequencies.

2 Materials and Methods

2.1 Chameleon Housing and Care

Chameleons were housed individually in large glass terrariums with heat lamps and ultraviolet (UV) light sources on a 12-hour day-night cycle. The cages were separated by an opaque partition to decrease or eliminate stress on the animals, as *C. calyptratus* are quite territorial. They were fed a diet of five, engorged crickets (fed a diet of sweet potatoes and cricket food) and watered three times a day by a MistKing Ultimate Misting System.

2.2 Electrode Construction

Bipolar hook electrodes were constructed with formvar-insulated nichrome wire (0.0020" bare and 0.0026" coated A-M Systems). Electrodes were comprised of two wires glued at their terminal ends with veterinary-grade cyanoacrylate. The wires were then threaded through a 27-gauge hypodermic needle. One millimeter of insulation was removed from the glued tips, and the wires bent away from each other in an arrowhead shape according to Anderson & Deban (2012). The constructed electrodes were autoclaved prior to surgery.

2.3 Surgery

The following protocol was approved by The University of South Dakota IACUC (AUP 17-12). Chameleons were anesthetized in an induction chamber with 5% isoflurane/1L O₂/minute and then placed in a mask receiving the same concentration of isoflurane throughout the surgical procedure. The chameleon

was positioned on its left side on a stage under a dissecting microscope. Electrodes were then implanted, via a hypodermic needle, into the *Mm. levator scapulae* (Figure 4), *M. sternohyoideus superficialis* (Figure 5), *M. sternohyoideus profundus* (Figure 5), *Mm. mandibulohyoideus* (Figure 5), *Mm. triceps* control muscle (Figure 6), and under the skin as a reference (Figure 6), a baseline for measurement by other electrodes. Veterinary-grade cyanoacrylate was applied to the implantation site securing the electrodes in place. The electrode wires were held together using rubber cement, approximately five centimeters from their implantation site along the remaining length of the nichrome wire. As the individual fully recovered from anesthesia, one millimeter of insulation was removed from the end of the electrodes and soldered to a plug (Anderson & Deban 2012). The plug and accelerometer were attached to a differential amplifier and PowerLab16/35 (ADInstruments; Dunedin, New Zealand) to record EMG and accelerometry data in LabChart V8.1.6 (ADInstruments; Dunedin, New Zealand).

2.4 EMG and Accelerometry

Chameleons were placed on a 12.7 mm-diameter wooden dowel after surgical recovery was complete, and the accelerometer was attached to their casque with beeswax (Figure 7). Biotremors were elicited in an antipredator context via the perceived physical threat of a syringe prodding the elbow. The forelimb that was not implanted with the control electrode was used to avoid any accidental stimulation of the implanted electrode in the *Mm. triceps*. This was repeated for six individuals, three males and three females. Chameleons were

then anesthetized after trials to surgically verify the integrity of electrode implantation.

2.5 Statistical analysis

The biotremors and EMG data were analyzed for correlation, latency to onset and offset (the time between muscle activation or cessation and biotremor production and termination), and effects of individual muscles or interactions between muscles on the duration of the biotremor. A total of 186 biotremors with corresponding EMG data were recorded from six individuals, three males and three females. Due to a limited number of test subjects, the experimental design of this project was such that repeated measures were taken from each individual. Therefore, these data do not satisfy the independence of observations assumptions of parametric analyses, so I included a random-effect parameter in my mixed effects linear models to account for all variation associated with the six individuals that were analyzed. Further, to account for violation of the normality assumption, I used a non-parametric resampling procedure for my comparison of frequencies between the sexes. The number of EMG recordings for each muscle is different due to the removal of electrodes by some individuals during some trials, which resulted in differing degrees of freedom (df) for all statistical analyses that incorporated all 186 observations of each muscle. An alpha value of 0.05 was used for all statistical analyses.

The correlation analyses were performed using linear regressions of the biotremors and the muscle electrical activity. To correlate which muscles were

generally responsible for the biotremor, durations (seconds) were used. Peak amplitude of the electrical activity of the muscles and biotremors were regressed to determine which muscles were responsible for the peak amplitude of the biotremor. The regression of the peak amplitudes provided a more precise picture of which muscles are most responsible because it is a specific point in time during the biotremor, rather than an entire biotremor.

Mixed-effect linear models were performed using the *lme4* (Bates *et al.* 2015) and *car* (Fox and Weisberg 2011) packages in R (R Core Team 2013). Mixed-effect linear models were created to describe which muscle contributed the most to the variation observed in the duration and peak amplitude of the biotremors. The model selection frameworks, Akaike's Information Criterion (AIC), Corrected Akaike's Information Criterion (AICc) and Bayesian Information Criterion (BIC), were used to evaluate how well each model explained the variation in the duration and time of peak activity in the biotremors. 'Individual' was included in the model as a random effect parameter to account for any variation attributed to the individuals, as there were repeated measures for all six individuals. The durations and peak amplitudes of the *Mm. levator scapulae* (LS), *M. sternohyoideus superficialis* (SH), *M. sternohyoideus profundus* (ST), and *Mm. mandibulohyoideus* (MH) were included as fixed-effect parameters in the models. An analysis of variance, using the *lmerTest* package (Kuznetsova *et al.* 2017), partitioned the variance to each parameter to determine the most important muscles responsible for the change in the duration and the peak amplitude of the biotremors. Muscles were then removed from the model in a

step-wise manner to determine which muscles most influenced the variation in biotremor duration, or if a model with fewer parameters best explained the variation within the biotremors. Models that included less than three parameters or a single interaction between two parameters were less explanatory than the additive, full, and three parameter models, except for the single parameter model 'ST' in the duration model comparisons. All other one and two parameter models were thus excluded from further analyses.

To illuminate any sexual dimorphism of biotremor frequency, a non-parametric resampling procedure was used in R to generate 10,000 random means calculated from the observed difference in means. Randomly generated means were used to create a normal distribution with which to compare our observed difference in means. This procedure was used because it is more conservative than parametric analyses, and it accounts for the non-normal distribution of the data.

3 Results

3.1 Correlation of Muscular Electrical Activity and Biotremor Activity

The durations of muscular electrical activity were correlated with the biotremor duration (Table 1; Figures 8-11). The *M. sternohyoideus superficialis* duration most strongly correlated ($r^2 = 0.9644$; $p = <0.001$), the *Mm. levator scapulae* the least correlated ($r^2 = 0.5744$; $p = <0.001$), and the *Mm. triceps* control was not correlated to biotremor duration ($r^2 = 0.0022$; $p = 0.24$). The times of peak muscular amplitude were strongly correlated with the times of the peak biotremor amplitudes (Table 2; Figures 13-16), with the time of peak activity in the *M. sternohyoideus superficialis* most correlated with the times of the biotremor peak amplitudes ($r^2 = 0.9962$; $p = <0.001$). The *Mm. triceps* durations were not associated with the biotremors ($p = 0.24$). The *Mm. triceps* activity was attributed to movement of the individuals during the prodding of the elbow.

3.2 Mechanistic Description

The latencies to onset and offset of the muscles were calculated using the mean time of activation and cessation in relation to the biotremors. For latency to onset, negative numbers indicate activity before the biotremor activation, and conversely, for latency to offset, negative numbers indicate activity after biotremor cessation. The mean latencies to onset and offset are *M. sternohyoideus superficialis* (onset = 0.016 seconds and offset = 0.075 seconds), *M. sternohyoideus profundus* (onset = 0.014 seconds and offset = - 0.137 second) *Mm. mandibulohyoideus* (onset = - 0.040 seconds and offset = - 0.011

seconds) *M. levator scapulae* (onset = - 0.196 seconds and offset = - 0.045 seconds), and *Mm. triceps* (onset = 0.021 and offset = - 0.682).

The calculated latency to onset and offset depict the mechanistic interactions of the muscles before, during, and after the biotremor (Figure 17). The *M. levator scapulae* and *Mm. mandibulohyoideus* activated prior to the biotremor onset, and the *M. sternohyoideus profundus* and *M. sternohyoideus superficialis* activated after the biotremor onset. The *M. sternohyoideus superficialis* then ceased activity prior to vibration cessation, and the *M. sternohyoideus profundus*, *Mm. mandibulohyoideus*, and *M. levator scapulae* ceased activity after the vibration had ended.

Linear mixed-effect regression model comparisons (AIC/AICc/BIC) for biotremor duration indicate that model 'ST' best explains the observed variation in biotremor duration, when compared to all other models (Table 4). An analysis of variance of model 'ST' shows that the *M. sternohyoideus profundus* explains the most variation in the duration of the biotremor ($p < 0.001$; Table 5).

Linear mixed-effect regression model comparisons (AIC/AICc/BIC) for peak amplitude of the biotremor indicate that model 'No ST' best explains the observed variation in biotremor peak amplitude, when compared to all other models (Table 6). An analysis of variance of model 'No ST' shows that the *M. sternohyoideus superficialis* explains the most variation in the peak amplitude of the biotremor ($p < 0.001$; Table 7). The *Mm. mandibulohyoideus* was also a significant contributor to the variation in peak amplitude ($p = 0.02$; Table 7).

3.3 Sexual Dimorphism

As demonstrated in Table 9, the mean female biotremor frequency (153.96 Hz) was significantly different ($p < 0.001$; Figure 19) than the mean male biotremor frequency (132.58 Hz). An analysis of variance and post-hoc Tukey HSD test (Table 10) indicated that there was a significant difference between the biotremor frequencies of male one and male two ($p < 0.001$), male two and male three ($p = 0.02$), but not between male one and male three ($p = 0.29$). Females were not significantly different. Figure 20 demonstrates that the difference in biotremor frequency observed in the males may be due to the size of the individuals.

4. Discussion

4.1 Correlation of Biotremor and Muscles

Chameleon biotremors have been cited in the literature and anecdotally reported by chameleon enthusiasts for decades (Brygoo 1971; Hillenius 1986; Tilbury 1992; Barnett *et al.* 1999). My results establish that the *M. sternohyoideus superficialis*, *M. sternohyoideus profundus*, *Mm. mandibulohyoideus*, and *Mm. levator scapulae* are responsible for the production of the biotremors in an antipredator response. This is demonstrated by linear regressions of durations and times of peak amplitudes (Figures 8-16; Tables 1-2), calculated latency to onset and offset, and linear mixed-effect regression models (Tables 4-7).

These results have partially supported the hypotheses of Boka (2012) and Huskey (unpublished) that biotremors were produced by the muscles surrounding the trachea and gular pouch; however, the role of the gular pouch in this mechanism is not yet understood. It is possible that the gular pouch is only employed during biotremors that are used for intraspecific communication, where the gular pouch amplifies the biotremor and allows the signal to travel farther. The presence of audible hoots is the only tangible evidence for this amplification by the gular pouch. Since no audible hoots were heard during our trials, I hypothesize that the gular pouch is not used during antipredator biotremor production. Courtship, territoriality, and antipredator trials accompanied by EMG, accelerometry, and the possible use of multi-detector row computed tomography (Salto *et al.* 2003), which can create 3-D data sets from moving organs, are necessary to explicitly demonstrate that the gular pouch is involved in the

mechanism of biotremor production in these contexts. Further studies are also necessary to validate that the same muscles involved in an anti-predator response are employed in intraspecific communication. However, it is also conceivable that a different combination of muscles is involved in the production of biotremors for intraspecific communication.

4.2 Mechanistic Description

The latency to onset and offset data suggest that the *M. levator scapulae* is activated prior to the biotremor to lengthen the ventral hyoid muscles by drawing the head back. The *Mm. mandibulohyoideus* and *M. sternohyoideus profundus* are the supporting cast in the production of biotremors as they act antagonistically against one another. The *M. sternohyoideus superficialis*, which attaches to the caudal base of the hyoid bone, then contracts to produce a portion of the biotremor that results in its peak amplitude.

The pattern of muscular contractions illustrated by the latency to onset data is further supported by our linear mixed-effect regression models for duration and peak amplitude. The model that best describes the variation in the duration of the biotremors was model 'ST', which included the *M. sternohyoideus profundus*, but did not include the *Mm. levator scapulae*, *Mm. mandibulohyoideus*, and *M. sternohyoideus superficialis*. The fact that the inclusion of the *Mm. levator scapulae*, *Mm. mandibulohyoideus*, and *M. sternohyoideus superficialis* in the additive model did not lead to an improvement in the model's ability to explain the variation in the duration of the biotremors

suggests that they may have a more important role in the amplitude or frequency than duration. In other words, the *Mm. levator scapulae*, *Mm. mandibulothyoideus*, and *M. sternothyoideus superficialis* contribute in no substantial way to variation in timing of the biotremor, and thus contribute little to the changes in biotremor duration in comparison to the *M. sternothyoideus profundus*.

The importance of the *M. sternothyoideus superficialis* is supported by our linear mixed-effect regression models that describe the variation in the time of peak amplitude of the biotremors. The model that best explained the time of peak amplitude variation was model 'No ST', which includes the *M. sternothyoideus superficialis*. The inclusion of the *M. sternothyoideus superficialis* in the model suggests that the peak amplitude of the biotremor cannot be achieved without this muscle. The analysis of variance of model 'No ST' also demonstrated that the *M. sternothyoideus superficialis* explained the most variation in peak amplitude, with the *Mm. mandibulothyoideus* also significantly contributing to the peak amplitude.

A study with a larger sample size and including more muscles in the EMG analysis will yield a better understanding of the mechanistic interactions that produce these biotremors. More comprehensive muscular surveys would also be advantageous as I only sampled a handful of the muscles in the neck. It is possible that there are other muscles that are involved in this mechanism, though unlikely because I sampled the muscles most closely associated with the gular pouch.

The determination that the *M. sternohyoideus profundus*, *M. sternohyoideus superficialis*, and *Mm. mandibulohyoideus* are primarily responsible for the production of the biotremors will allow scientists to determine if its physiological properties (*i.e.*, super-contracting, slow-twitch, fast-twitch, etc.) are different than those of other muscles. Electrophysiology and histology will illuminate any differences, and the results will allow for analysis of museum specimens for the presence of a muscle or muscles with the same physiological characteristics. The existence of muscles with the same physiological characteristics may be an indication of the ability to produce biotremors.

4.3 Sexual Dimorphism

A cursory exploration of biotremor frequencies reveals that males have lower mean frequencies than females (Table 7), with greater variation among males than females (Table 8). The non-parametric comparison of means indicates a significant difference between the frequency of male and female biotremors (Figure 19; Table 7). There are a few outliers in the female data that may be due to the inconsistencies in defense response of the chameleons or inconsistent pressure while prodding the individuals. These results are congruent with the lengthy list of observed sexually-dimorphic traits and are likely a result of the size difference between males and females. The biotremors are a consequence of the *M. sternohyoideus superficialis* contracting, consequently those with a larger *M. sternohyoideus superficialis* will likely have a lower

frequency biotremor, which suggests that size may contribute to lower frequencies (Figure 20).

The variation among male biotremor frequencies may be driving sexual selection in *C. calypttratus*. This would require significant variation in frequency observed between individual males with the more fit individuals having a higher, lower, or intermediate frequency, depending on female preferences. This is specifically important because *C. calypttratus* have been documented using biotremors during courtship (Barnett *et al.* 1999). Barnett *et al.* (1999) also documented the exchange of biotremors between males during territoriality displays.

5 Conclusion

The present study is the first description of a biotremor producing mechanism in a reptilian species. The evidence produced here, in conjunction with the absence of a syrinx, vocal cords, and external ears (Wever 1968; Wever 1969a; Wever 1969b; Measey *et al.* 2009) paired with the theoretical ability to detect biotremors (Hartline 1971; Barnett *et al.* 1999) demonstrates that biotremors can be utilized by *C. calyptratus* for communication. However, the hearing abilities of *C. calyptratus* must be further described, regarding their ability to detect vibrations, before it can definitively be said that biotremors are employed for true communication. Further studies of other chameleon species will also reveal if this ability is ubiquitous among all chameleons, merely a behavior exhibited by a few species, or a novel adaptation in *C. calyptratus*.

6. References

- Anderson, C.V. & Deban, S.M. (2012) Thermal effects on motor control and in vitro muscle dynamics of the ballistic tongue apparatus in chameleons. *Journal of Experimental Biology*. 215:4345-4357.
- Barnett, K.E., Cocroft, R.B. & Fleishman, L.J. (1999) Possible communication by substrate vibration in a chameleon. *Copeia*. 1999:225-228.
- Bass, A.H. & Clark, C.K. (2003) The physical acoustics of underwater sound communication. *Acoustic Communication*. 16:15-64.
- Bates, D., Maechler, M., Bolker, B., Walker, S. (2015) Fitting Linear Mixed-Effects Models Using lme4. *Journal of Statistical Software*. 67(1):1-48.
- Beckers, G. J. L. (2011) Bird speech perception and vocal production: a comparison with humans. *Human Biology*. 83(2):191-212.
- Boka, K. (2012) "What's that hooting sound? A survey on novel sound producing mechanisms in chameleons". Honors Thesis—Western Kentucky University
- Bradburry, J.W. & Vehrencamp, S.L. (2011) *Principles of Animal Communication* (2nd edition). Sinauer Associates.
- Brygoo, E.R., (1971) Reptiles Sauriens Chamaeleonidae, genre Chamaeleo. *Faune de Madagascar*, 33:1-318.
- Elemans, C.P.H., Larsen, O.N., Hoffmann, M.R. & Van Leeuwen, J.L. (2003) Quantitative modeling of the biomechanics of the avian syrinx. *Animal Biology*. 53:183-193.
- Endler, J.A. (1993) Some general comments on the evolution and design of animal communication systems. *Philosophical Transactions of the Royal Society B: Biological Sciences*. 340:215-225.
- Fee, M.S., Shraiman, B., Persaran, B. & Mitra, P.P. (1998) The role of nonlinear dynamics of the syrinx in the vocalizations of a songbird. *Nature*. 395:67.
- Fine, M., Friel, J., McElroy, D., King, C., Loesser, K., Newton, S. (1997) Pectoral spine locking and sound production in the channel catfish *Ictalurus punctatus*. *Copeia*. 1997:777-790.
- Fine, M., Mallow, K., King, C., Mitchell, S., Cameron, T. (2001) Movement and sound generation by the toadfish swimbladder. *Journal of Comparative Physiology*. 187:371-379.

- Fox, J. & Weisberg, S. (2011) *An {R} Companion to Applied Regression*, Second Edition. Thousand Oaks CA: Sage.
URL: <http://socserv.socsci.mcmaster.ca/jfox/Books/Companion>
- Germershausen, G. (1913) Anatomische untersuchungen über den kehlkopf der chamaeleonen. *Sitzungsberichte der Gesellschaft naturforschender Freunde zu Berlin*. 191:462-535.
- Given, M.F. (1987) Vocalizations and acoustic interactions of the carpenter frog, *Rana vergatipes*. *Herpetologica*. 43:467-481.
- Glaw, F. (2015) Taxonomic checklist of chameleons (Squamata: Chamaeleonidae). *Vertebrate Zoology*. 65:167-246.
- Hartline, P.H. (1971) Physiological basis for detection of sound and vibration in snakes. *Journal of Experimental Biology*. 54:349-371.
- Heth, G., E. Frankenberg, A. Raz, and N. Nevo. (1987) Vibrational communication in subterranean mole rats (*Spalax ehrenbergi*). *Behavioral Ecology and Sociobiology*. 21:31-33.
- Hildebrand, M. & Goslow, G. (1985) *Analysis of Vertebrate Structure* (4th edition). John Wiley.
- Hill, P. S. M. & Wessel, A. (2016) Primer: biotremology. *Current Biology*. 26:181-191.
- Hillenius, D. (1986) The relationship of *Brookesia*, *Rhampholeon* and *Chamaeleo* (Chamaeleonidae, Reptilia). *Bijdragen tot de Dierkunde*. 56 (1):29-36.
- Huskey, S. (2017) *The Skeleton Revealed: An Illustrated Tour of the Vertebrates*. Johns Hopkins University Press.
- Kuznetsova, A., Brockhoff, P., Christensen, R. (2017) "lmerTest Package: Tests in linear Mixed Effects Models." *Journal of Statistical Software*. 82(13):1-26.
- Labra, A., Sufán-Catalan, J., Solis, R. & Penna, M. (2007) Hissing sounds by the lizard *Pristidactylus volcanensis*. *Copeia*. 1019-1023.
- Macedonia, J. & Evans, C. (1993) Essay on contemporary issues in ethology: variation among mammalian alarm call systems and the problem of meaning in animal signals. *Ethology*. 93(3):177-197

- Measey, G.J., Hopkins, K. & Tolley, K.A. (2009) Morphology, ornaments and performance in two chameleon ecomorphs: is the casque bigger than the bite? *Zoology*. 112:217-226.
- Moore, B. A., Russell, A.P. & Bauer, A. M. (1991) Structure of the larynx of the tokay gecko (*Gekko gecko*), with particular reference to the vocal cords and glottal lips. *Journal of Morphology*. 210:227-238.
- O'connell-Rodwell, C.E. (2007) Keeping an "ear" to the ground: Seismic communication in elephants. *Physiology*. 22:287-294.
- O'connell-Rodwell, C.E., Hart, L.A. & Arnason, B.T. (2001) Exploring the potential use of seismic waves as a communication channel by elephants and other large mammals. *American Zoologist*. 41:1157-1170.
- R Core Team (2013) R: A language and environment for statistical computing. R Foundation for Statistical Computing. Vienna, Austria. URL: <http://www.R-project.org/>.
- Raghavendra, B.N., Horii, S.C., Reede, D.L., Rumancik, W.M., Persky, M. & Bergeron, T. (1987) Sonographic anatomy of the larynx, with particular reference to the vocal cords. *Journal of Ultrasound Medicine*. 6:225-230.
- Salto, K., Salto, M., Komatu, S. & Ohtomo. (2003) Real-time four-dimensional imaging of the heart with multi-detector row CT. *RadioGraphics*. 23:1.
- Searcy, W.A. & Nowicki, S. (2012) *The Evolution of Animal Communication: Reliability and Deception Signaling Systems*. Princeton University Press.
- Smyth, T. & Smith, J.O. (2002) The sounds of the avian syrinx—Are they really flute like? *Proceedings of the 5th International Conference on Digital Audio Effects*. DAFX-02. 199-202.
- Tilbury, C.R. (1992) A new dwarf forest chameleon (Sauria: *Rhampholeon* Günther 1874) from Malawi, central Africa. *Tropical Zoology*. 5:1-9.
- Tolley, K. A. & Herrel, A. (2014) *The Biology of Chameleons*. University of California Press.
- Tornier, G. (1905) Bau und betätigung der kopflappen und halsluftsäcke bei chamäleon. *Zoologische jahrbücher abteilung für anatomie und ontogenese der tiere*. *Zoologische Jahrbuecher Abteilung fuer Anatomie und Ontogenie der Tiere*. 21:1-40.

- Wever, E.G. (1968) The ear of the chameleon: *Chamaeleo senegalensis* and *Chamaeleo quilensis*. *Journal of Experimental Zoology*. 168(4):423-436.
- Wever, E.G. (1969a) The ear of the chameleon: the round window problem. *Journal of Experimental Zoology*. 171:1-5.
- Wever, E.G. (1969b) The ear of the chameleon: *Chamaeleo hohnelii* and *Chamaeleo jacksonii*. *Journal of Experimental Zoology*. 171(3):305-312.
- Wilson, B., Batty, R.S. & Dill, L.M. (2004) Pacific and Atlantic herring produce burst pulse sounds. *Proceeding of the Royal Society B: Biological Sciences*. 271:95-97.

7. Tables

Table 1: The *M. levator scapulae*, *Mm. mandibulothyoideus*, *M. sternohyoideus profundus* (*M. sternothyroideus*), and *M. sternohyoideus superficialis* (*M. sternohyoideus*), mean duration (seconds), r^2 , Standard Error, t-values, F-statistics, degrees of freedom (df), and the associated p-values for the linear regression of biotremor duration and muscle electrical activity duration.

Muscle	Mean Duration (seconds)	r^2	Standard Error	t	F	df	p-value
Biotremor	0.2082	-	-	-	-	-	-
<i>M. sternohyoideus</i>	0.2251	0.8262	0.0537	19.04	362.3	75	<0.001
<i>M. sternothyroideus</i>	0.3057	0.9644	0.0256	38.280	1465	53	<0.001
<i>Mm. mandibulothyoideus</i>	0.2215	0.6816	0.0574	15.790	249.3	115	<0.001
<i>Mm. levator scapulae</i>	0.2264	0.5744	0.0790	12.765	163.0	119	<0.001
<i>Mm. triceps</i>	0.0020	0.0022	0.0088	-1.188	1.4	186	0.24

Table 2: Muscles, r^2 , Standard Error, t-values, F-statistics, degrees of freedom (df), and the associated p-values for the linear regression of time of peak activity of the biotremor and muscle electrical activity (V). The *Mm. levator scapulae* (LS), *Mm. mandibulohyoideus* (MH), *M. sternohyoideus profundus* (ST), and *M. sternohyoideus superficialis* (SH).

Muscle	r^2	Standard Error	t	F	df	p
<i>M. sternohyoideus</i>	0.9962	0.007607	130.715	17,090	64	<0.001
<i>M. sternothyroideus</i>	0.9944	0.01066	93.163	8679	48	<0.001
<i>Mm. mandibulohyoideus</i>	0.9910	0.009999	100.226	10,050	90	<0.001
<i>Mm. levator scapulae</i>	0.9952	0.007018	141.918	20,140	97	<0.001

Table 3: The time of *M. levator scapulae*, *Mm. mandibulohyoideus*, *M. sternohyoideus profundus* (*M. sternothyroideus*), and *M. sternohyoideus superficialis* (*M. sternohyoideus*) activation and cessation in relation to the biotremor activation, peak activity, and offset. Active muscles, peak activity, and biotremor activity are indicated by an X and no activity is indicated by --. Time 0.00 is the start of the biotremor.

Muscle	-0.19 seconds	-0.04 seconds	0.00 seconds	0.01 seconds	0.02 seconds	0.05 seconds	0.08 seconds	0.09 seconds	0.13 seconds	0.22 seconds
Biotremor	--	--	X	X	X	X	X	--	--	--
Peak Biotremor Amplitude	--	--	--	--	X	--	--	--	--	--
<i>M. sternohyoideus</i>	--	--	--	--	X	X	--	--	--	--
<i>M. sternothyroideus</i>	--	--	--	X	X	X	X	X	X	--
<i>Mm. mandibulohyoideus</i>	--	X	X	X	X	X	X	--	--	--
<i>Mm. levator scapulae</i>	X	X	X	X	X	X	X	X	--	--

Table 4: The models created to explain the variation in biotremor duration, including the model, parameters, degrees of freedom (df), AIC, AICc and BIC values. The *M. levator scapulae*(LS), *Mm. mandibulohyoideus* (MH), *M. sternohyoideus profundus* (ST), and *M. sternohyoideus superficialis* (SH) are the model parameters.

Model	Model	df	AIC	AICc	BIC
Full	SH x ST x MH x LS x IND	13	-148.5	-147.2	-122.1
Additive	SH + ST + MH + LS + IND	7	-118.4	-118.1	-108.1
No ST	SH + MH + LS +IND	6	-212.9	-212.7	-199.4
No MH	SH + ST + LS + IND	6	-116.2	-115.9	-107.4
No SH	ST + MH + LS + IND	6	-224.2	-223.9	-212.3
No LS	ST + SH + MH + IND	6	-138.2	-137.9	-129.0
ST	ST + IND	4	-249.9	-249.8	-241.9

Table 5: The result of an analysis of variance of the muscle included in the model that best described the variation in biotremor duration according to both AIC, AICc, and BIC, with the corresponding degrees of freedom (df), sum of squares (SS), mean squares (MS), F-value, and p-values for the *M. sternohyoideus profundus* (ST).

Model parameter	df	SS	MS	F	p-value
ST	1	1.07	1.07	3069.4	<0.001

Table 6: The models created to explain the variation in biotremor peak amplitude, including the model, parameters, degrees of freedom (df), AIC, AICc and BIC values. The *M. levator scapulae*(LS), *Mm. mandibulohyoideus* (MH), *M. sternohyoideus profundus* (ST), and *M. sternohyoideus superficialis* (SH) are the model parameters.

Model	Model	df	AIC	AICc	BIC
Full	SH x ST x MH x LS x IND	13	-147.5	-147.2	-128.5
Additive	SH + ST + MH + LS + IND	7	-67.1	-66.7	-56.8
No ST	SH + MH + LS +IND	6	-149.6	-149.4	-136.0
No MH	SH + ST + LS + IND	6	-63.9	-63.7	-55.1
No SH	ST + MH + LS + IND	6	-85.6	-85.4	-73.8
No LS	ST + SH + MH + IND	6	-73.1	-72.9	-63.9

Table 7: The results of an analysis of variance of the muscles included in the model that best described the variation in biotremor peak activity according to both AIC, AICc, and BIC, with the corresponding degrees of freedom (df), sum of squares (SS), mean squares (MS), F-value (F), and p-values. The *M. levator scapulae*(LS), *Mm. mandibulohyoideus* (MH), and *M. sternohyoideus superficialis* (SH) are the model parameters.

Model parameters	df	SS	MS	F	p-value
SH	1	0.06	0.06	11.96	<0.001
MH	1	0.03	0.03	5.54	0.02
LS	1	0.01	0.01	0.94	0.34

Table 8: Sex, number of individuals (n), the mean biotremor frequencies (Hz), Variance, and Standard Deviation of male and female biotremor frequencies.

Sex	n	Mass (g)	Mean Biotremor Frequency (Hz)	Variance	Standard Deviation
Male (means)	112	178	132.58	597.0	24.43
Male One	33	202	146.9	091.1	09.6
Male Two	58	256	122.7	686.0	26.2
Male Three	21	76	137.7	555.7	23.6
Female (means)	74	133.8	153.96	3640.8	60.34
Female One	30	117	149.1	75.9	8.7
Female Two	39	147.5	158.9	6877.1	82.9
Female Three	5	137	145.1	48.0	6.9

Table 9: The results of t-tests between males. Lower and upper Confidence intervals (CI) and the corresponding p-values.

Individual Comparisons	Lower CI	Upper CI	p
Male One: Male Two	-35.6	-12.8	<0.001
Male Three: Male One	23.7	5.3	0.29
Male Two: Male Three	1.9	28.1	0.021

8. Figures

Figure 1: The left side of a *C. calypttratus* trachea with a gular pouch (A) and of a *Trioceros jacksonii xantholophus* trachea without a gular pouch (B).



Figure 2: Images illustrating the diversity of the gular pouches from *C. calyptratus*, *C. gracilis*, *T. melleri*, *C. dilepis*, and *Furcifer verrucosus*.

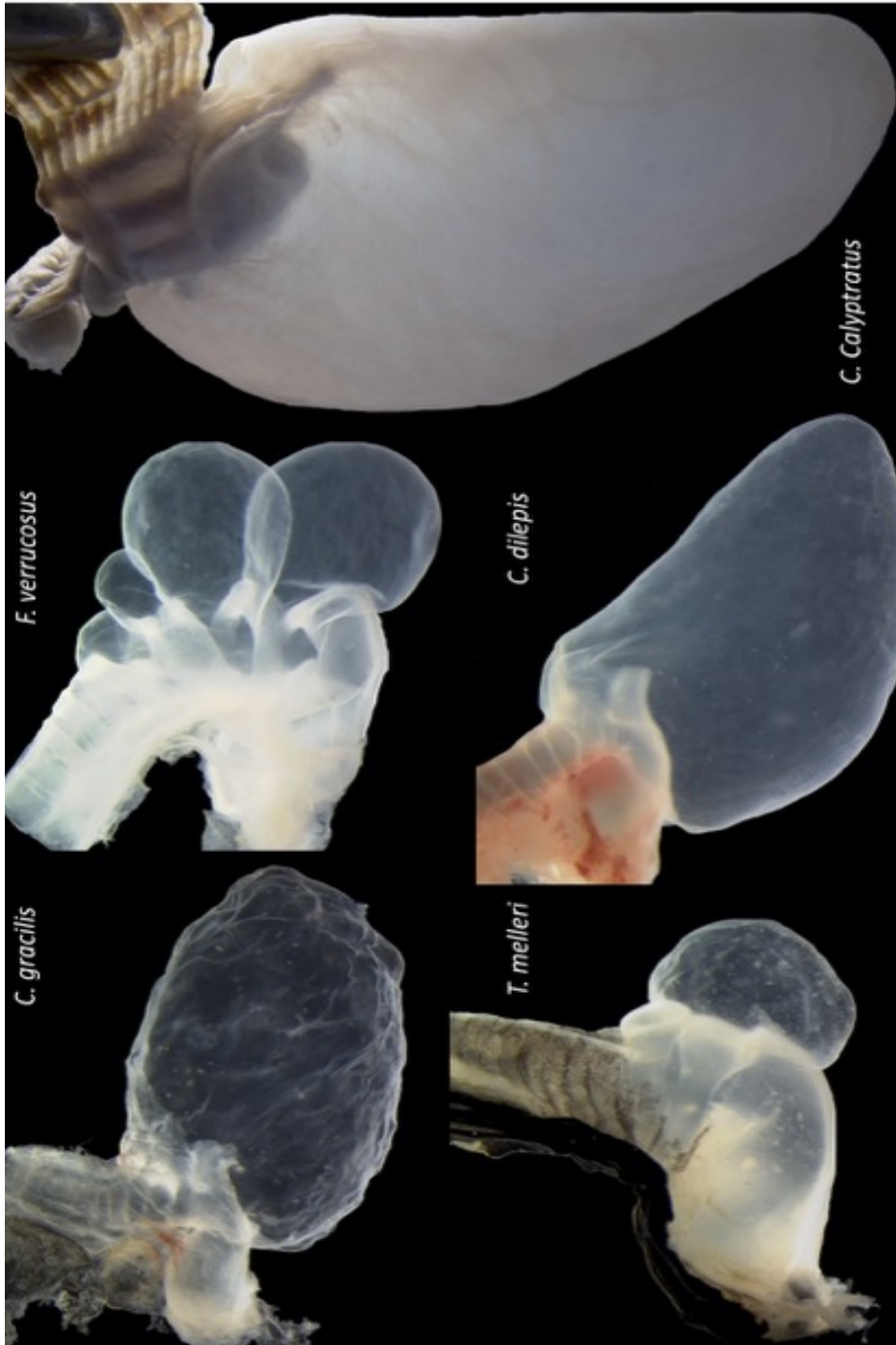


Figure 3: Lateral view of a male *C. calypttratus* illustrating the tight association between the gular pouch (a) and the *Mm. mandibulothyoideus* (b), *M. sternothyoideus superficialis* (c), *M. sternothyoideus profundus* (d).

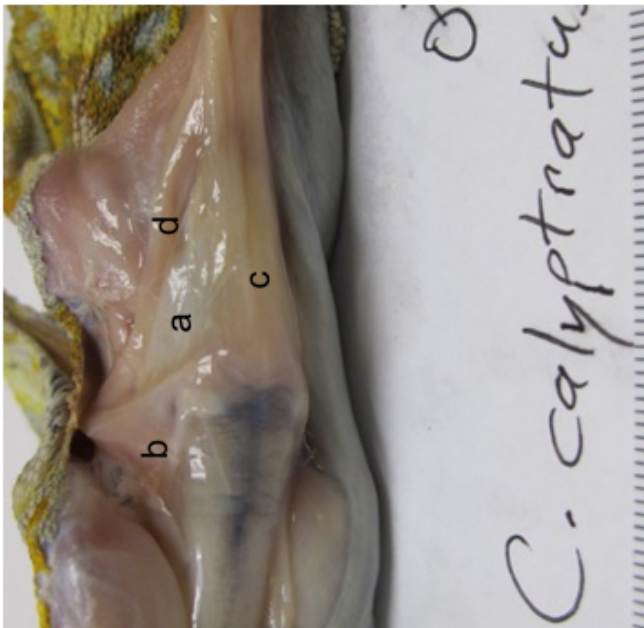
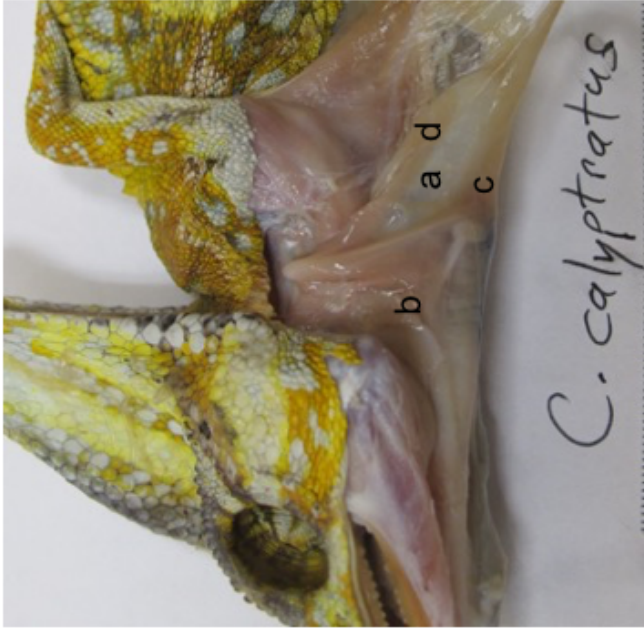


Figure 4: Electrode implanted into the *Mm. levator scapulae* and its location in relation to the ceratobranchial and *Mm. mandibulohyoideus*.

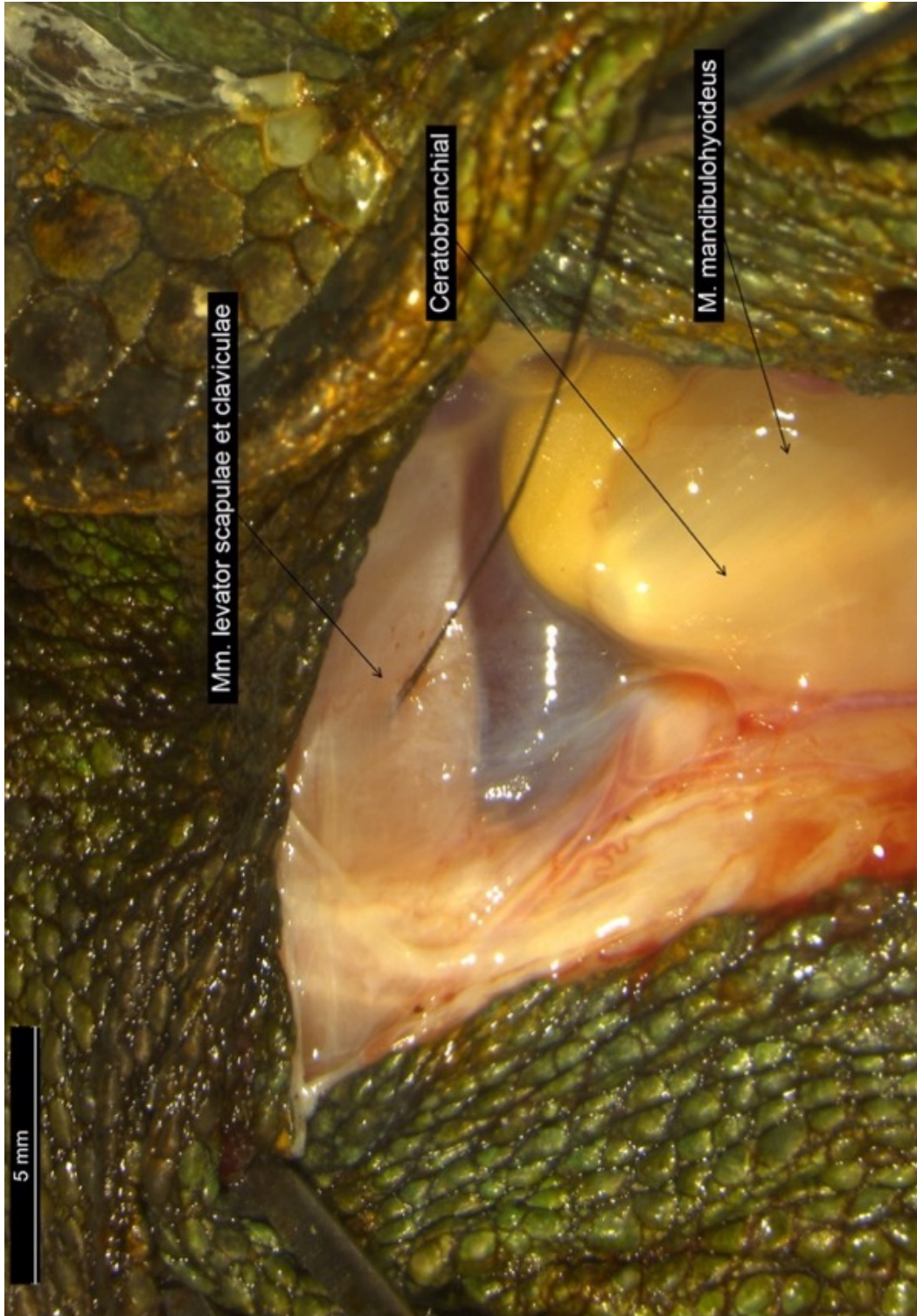


Figure 5: Electrodes implanted in the *Mm. sternohyoideus superficialis*, *Mm. sternohyoideus superficialis et profundus*, and *Mm. mandibulohyoideus* and their location in relation to the gular pouch and ceratobranchial.

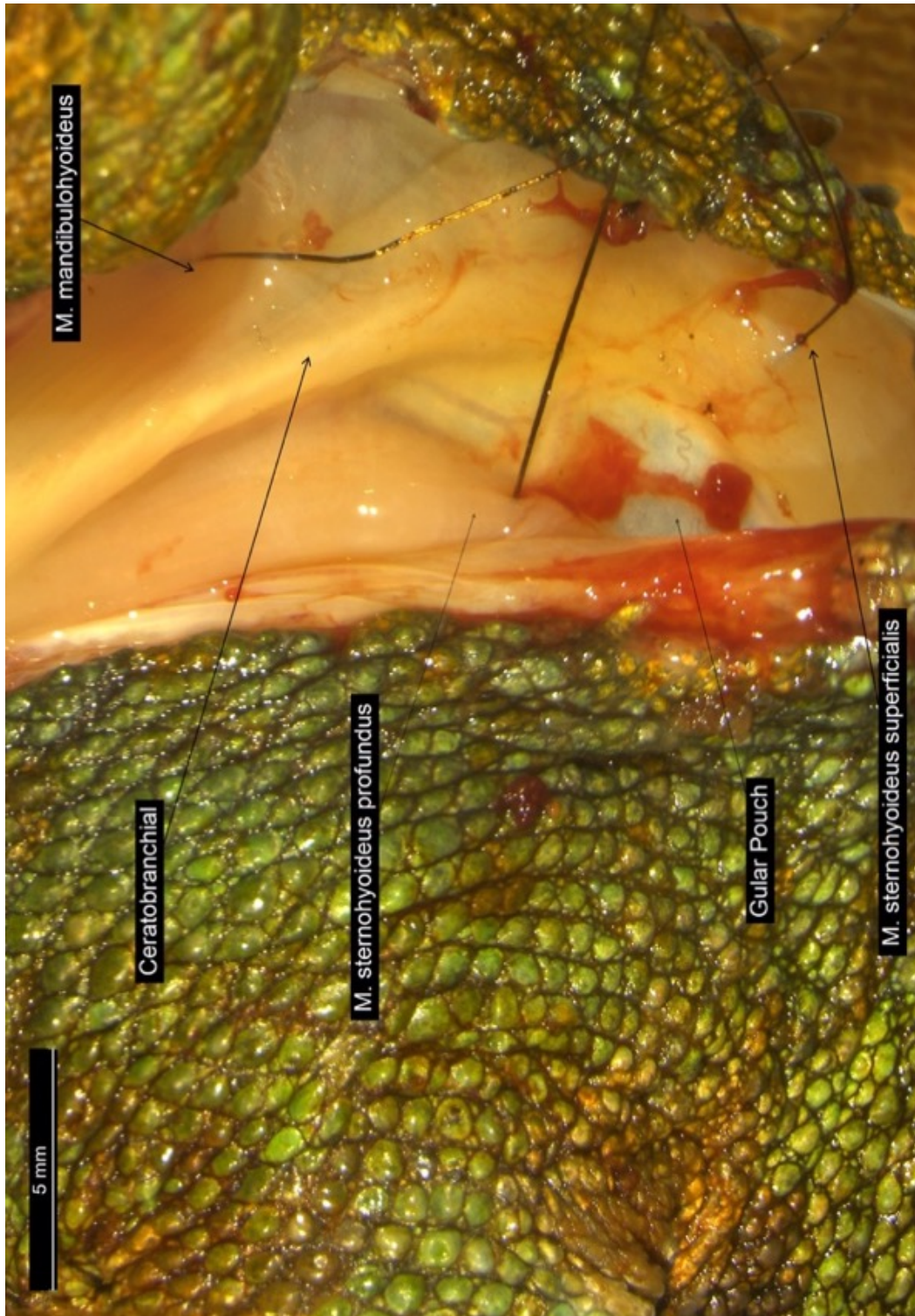


Figure 6: electrodes implanted into the *Mm. triceps* (control electrode) and the reference under the skin.

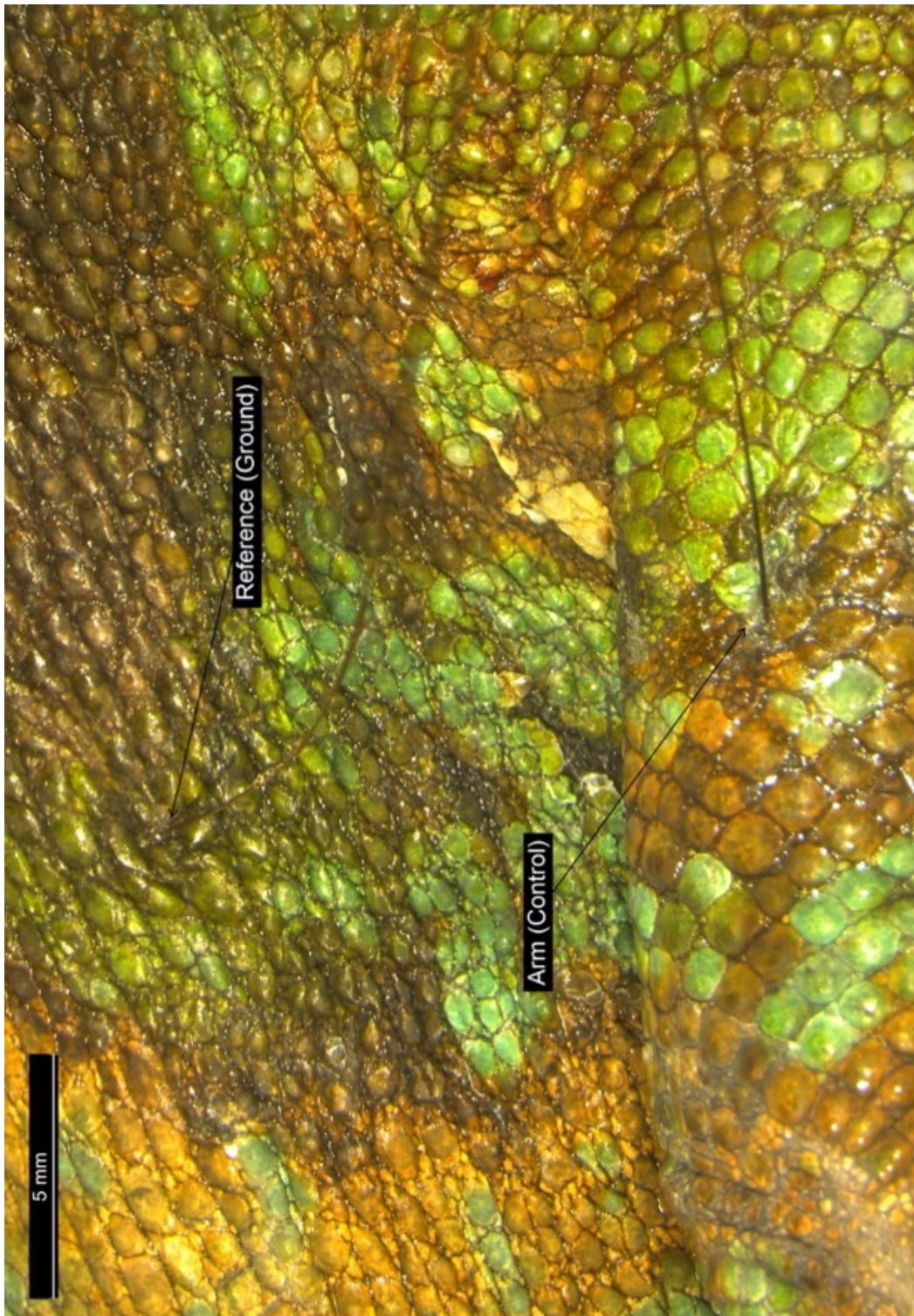


Figure 7: A male *C. calypttratus* (post-surgery) on a 12.7 mm dowel with an accelerometer attached to the casque with beeswax.

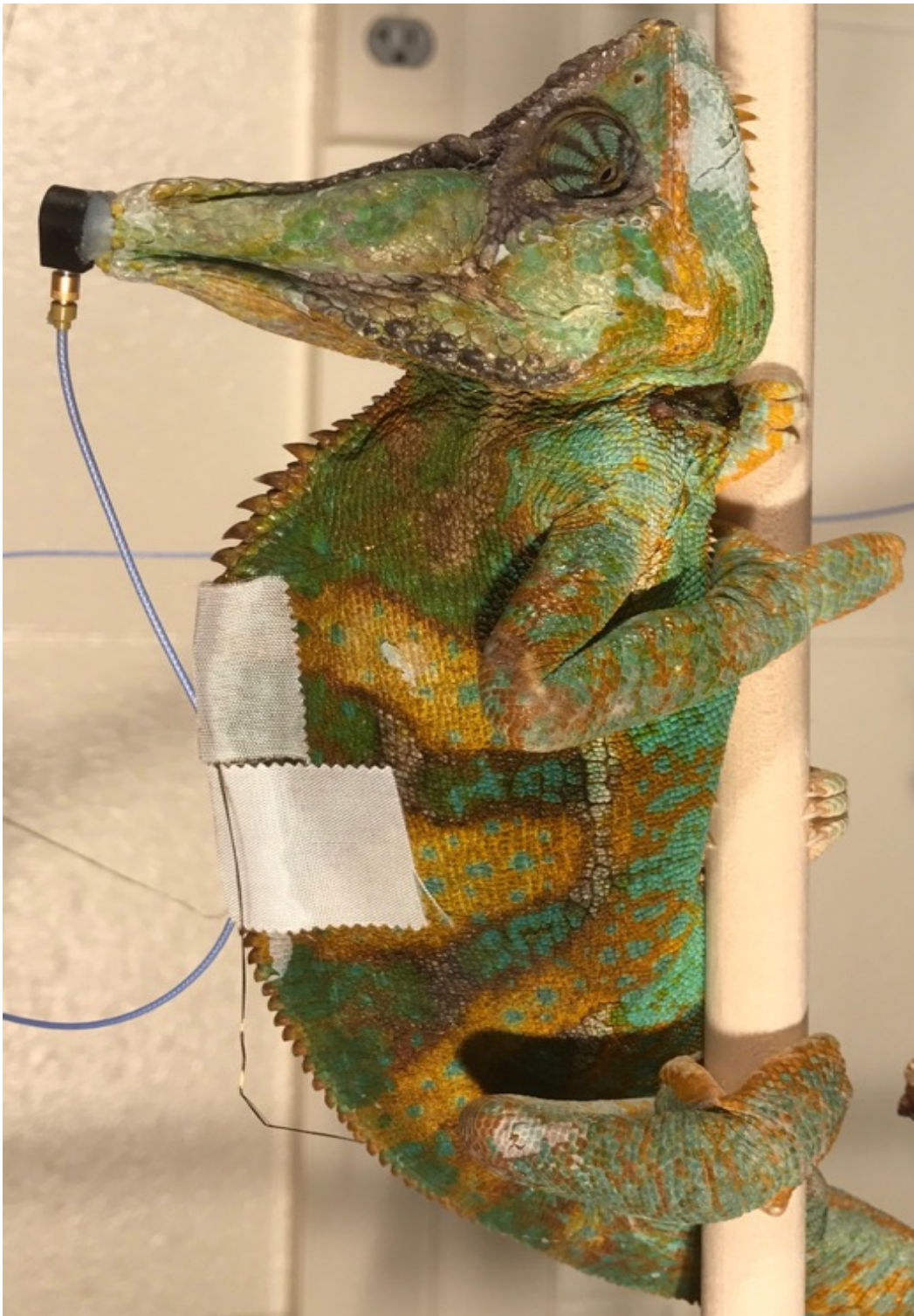


Figure 8: A linear regression of the duration of *Mm. sternohyoideus superficialis* electrical activity and the duration of the biotremor. The axes are labeled in seconds, and blue circles indicate the duration of a single recorded biotremor and the corresponding duration of the muscular electrical activity. The black line is the line of best fit.

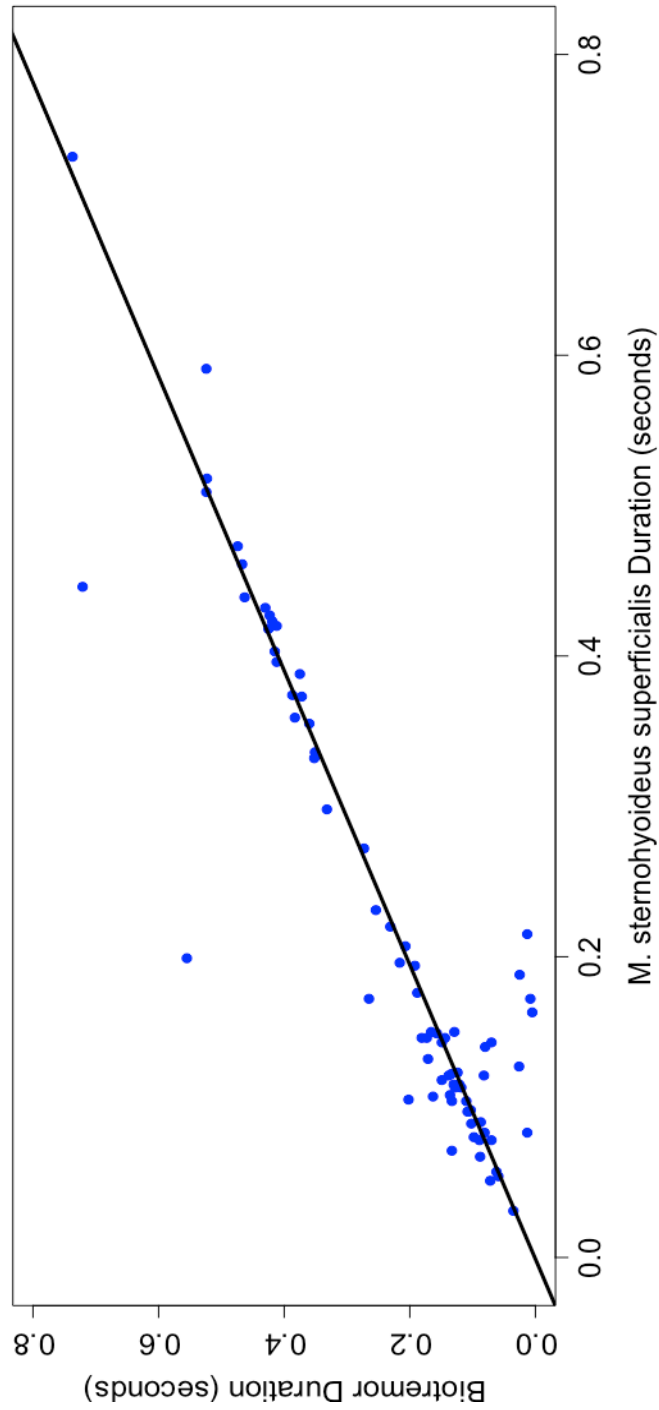


Figure 9: A linear regression of the duration of *Mm. sternohyoideus profundus* electrical activity and the duration of the biotremor. The axes are labeled in seconds, and blue circles indicate the duration of a single recorded biotremor and the corresponding duration of the muscular electrical activity. The black line is the line of best fit.

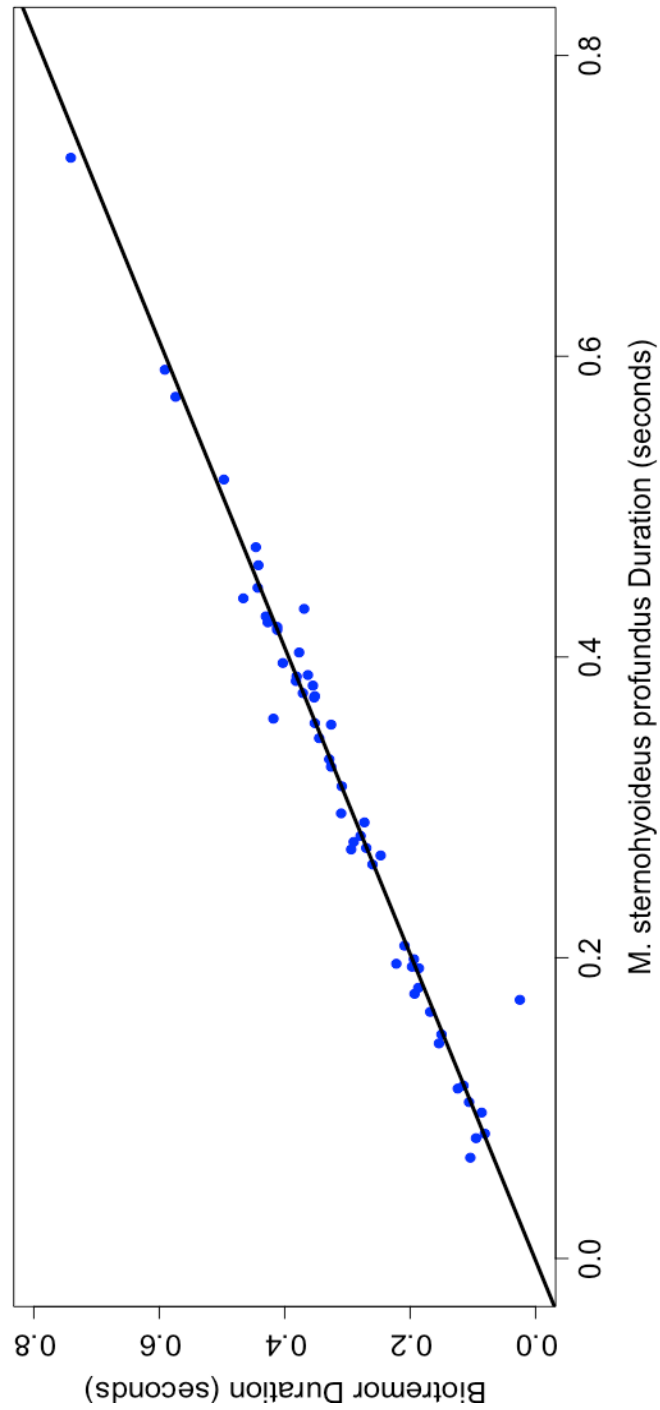


Figure 10: A linear regression of the duration of *Mm. mandibulothyoideus* electrical activity and the duration of the biotremor. The axes are labeled in seconds, and blue circles indicate the duration of a single recorded biotremor and the corresponding duration of the muscular electrical activity. The black line is the line of best fit.

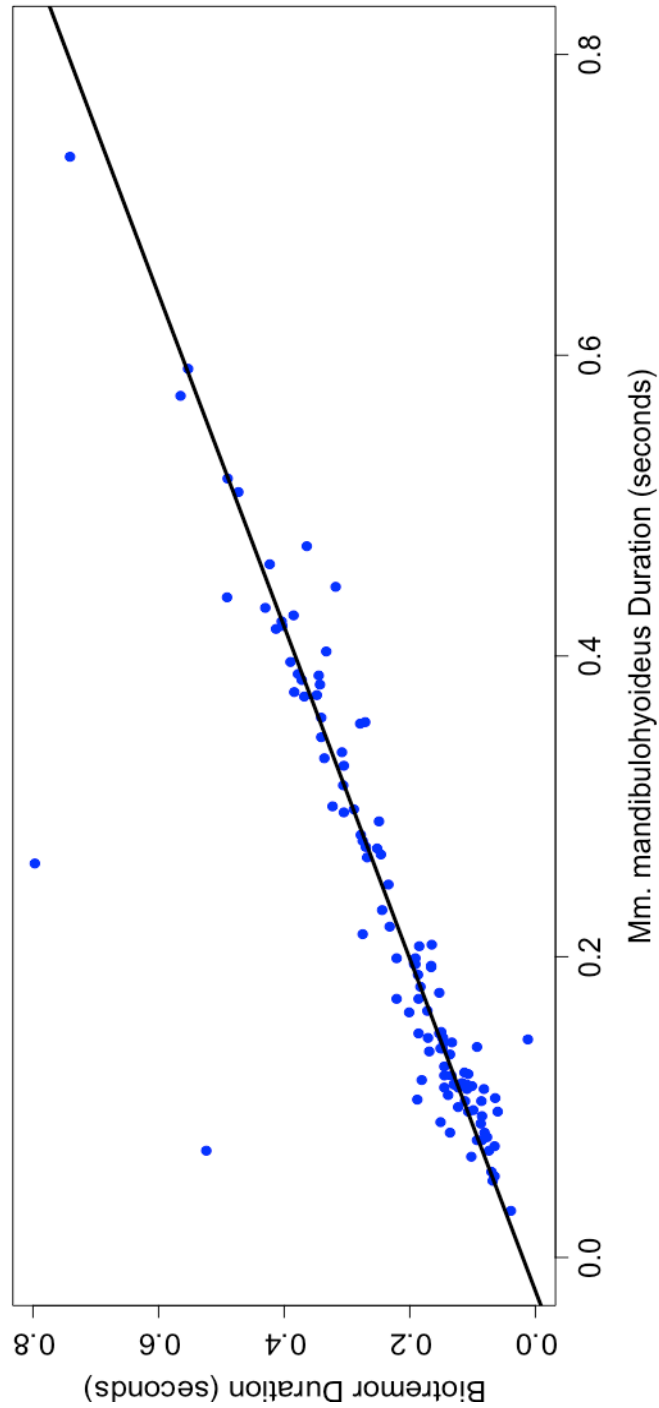


Figure 11: A linear regression of the duration of *Mm. levator scapulae* electrical activity and the duration of the biotremor. The axes are labeled in seconds, and blue circles indicate the duration of a single recorded biotremor and the corresponding duration of the muscular electrical activity. The black line is the line of best fit.

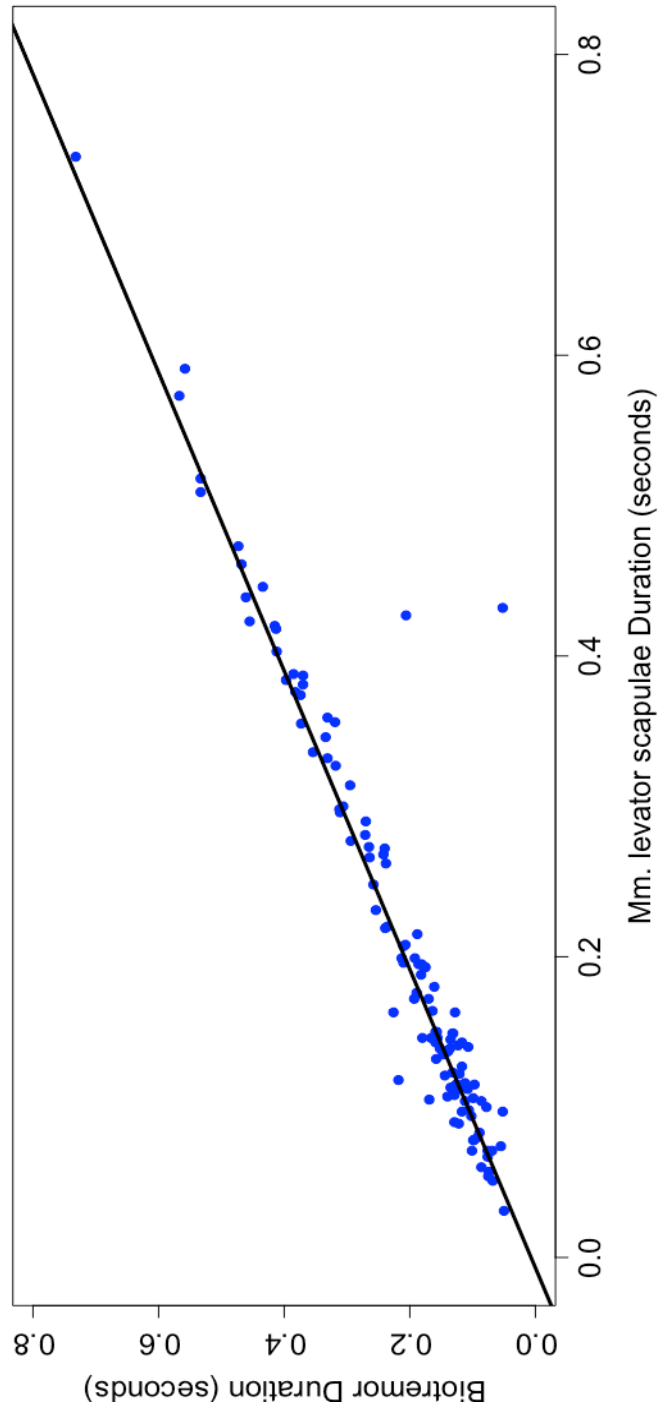


Figure 12: A linear regression of the duration of *Mm. triceps* electrical activity and the duration of the biotremor. The axes are labeled in seconds, and blue circles indicate the duration of a single recorded biotremor and the corresponding duration of the muscular electrical activity. The black line is the line of best fit.

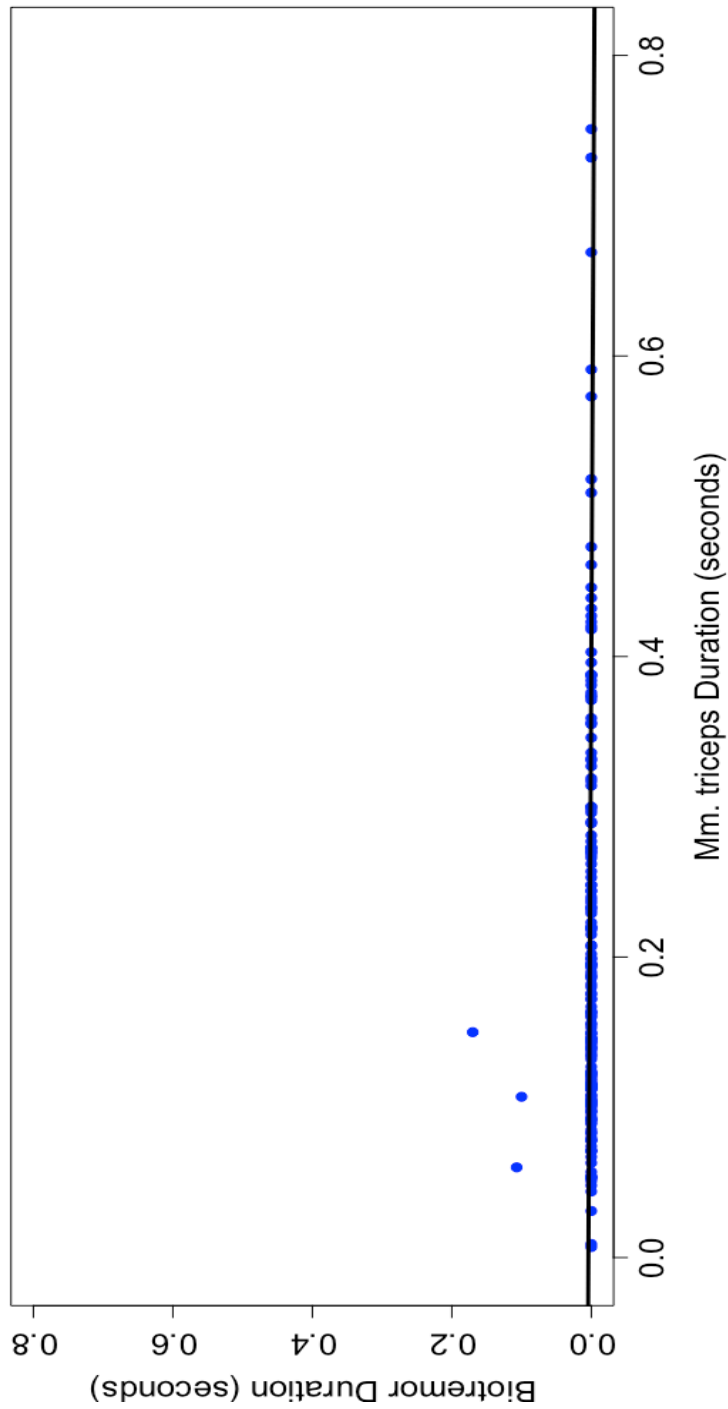


Figure 13: A linear regression of the peak *M. sternohyoideus superficialis* electrical activity and the peak activity of the biotremor. The axes are labeled in seconds, and blue circles indicate the time of a single recorded peak activity of the biotremor and the corresponding time of peak muscular electrical activity. The black line is the line of best fit.

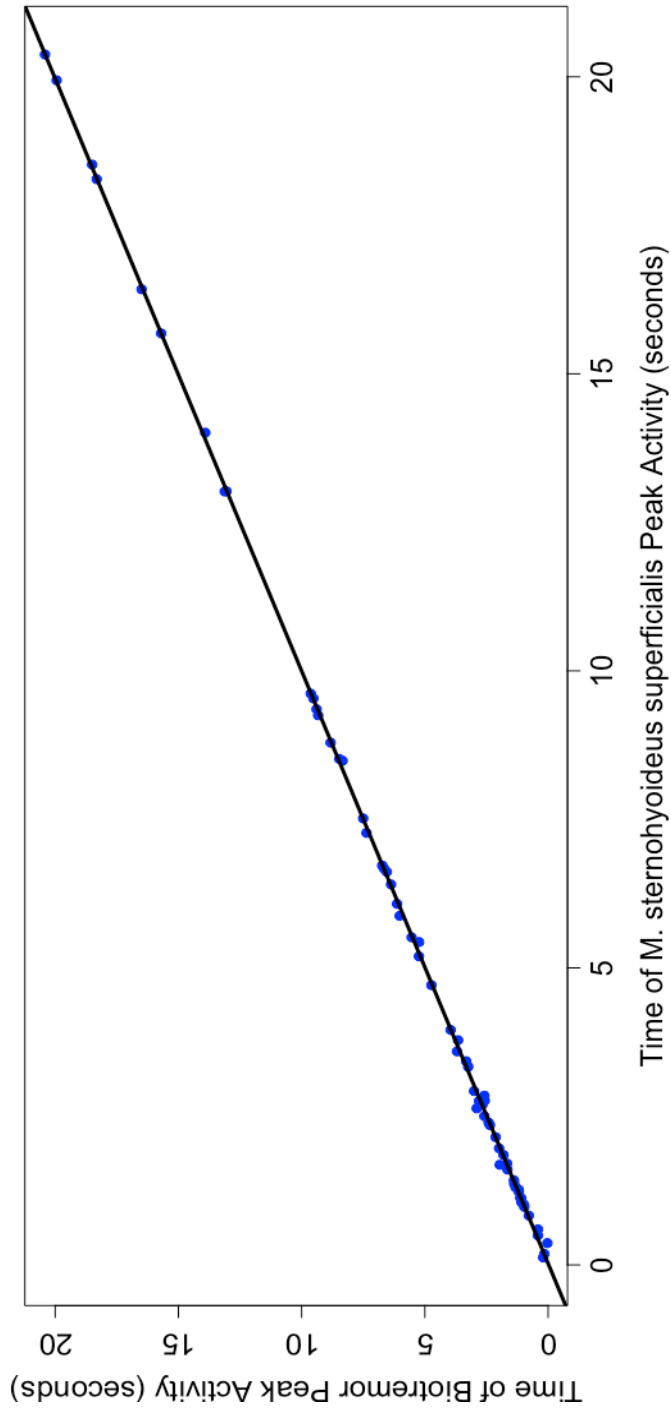


Figure 14: A linear regression of the peak *M. sternohyoideus profundus* electrical activity and the peak activity of the biotremor. The axes are labeled in seconds, and blue circles indicate the time of a single recorded peak activity of the biotremor and the corresponding time of peak muscular electrical activity. The black line is the line of best fit.

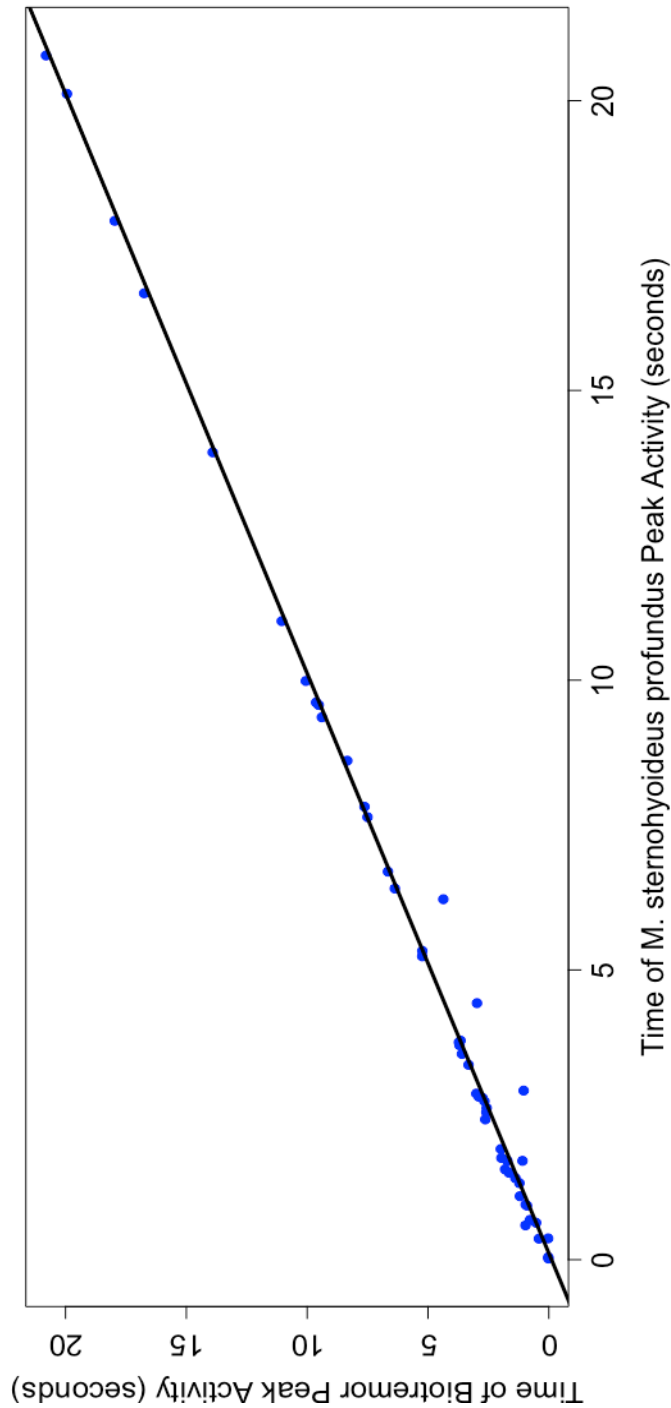


Figure 15: A linear regression of the peak *Mm. mandibulothyoideus* electrical activity and the peak activity of the biotremor. The axes are labeled in seconds, and blue circles indicate the time of a single recorded peak activity of the biotremor and the corresponding time of peak muscular electrical activity. The black line is the line of best fit.

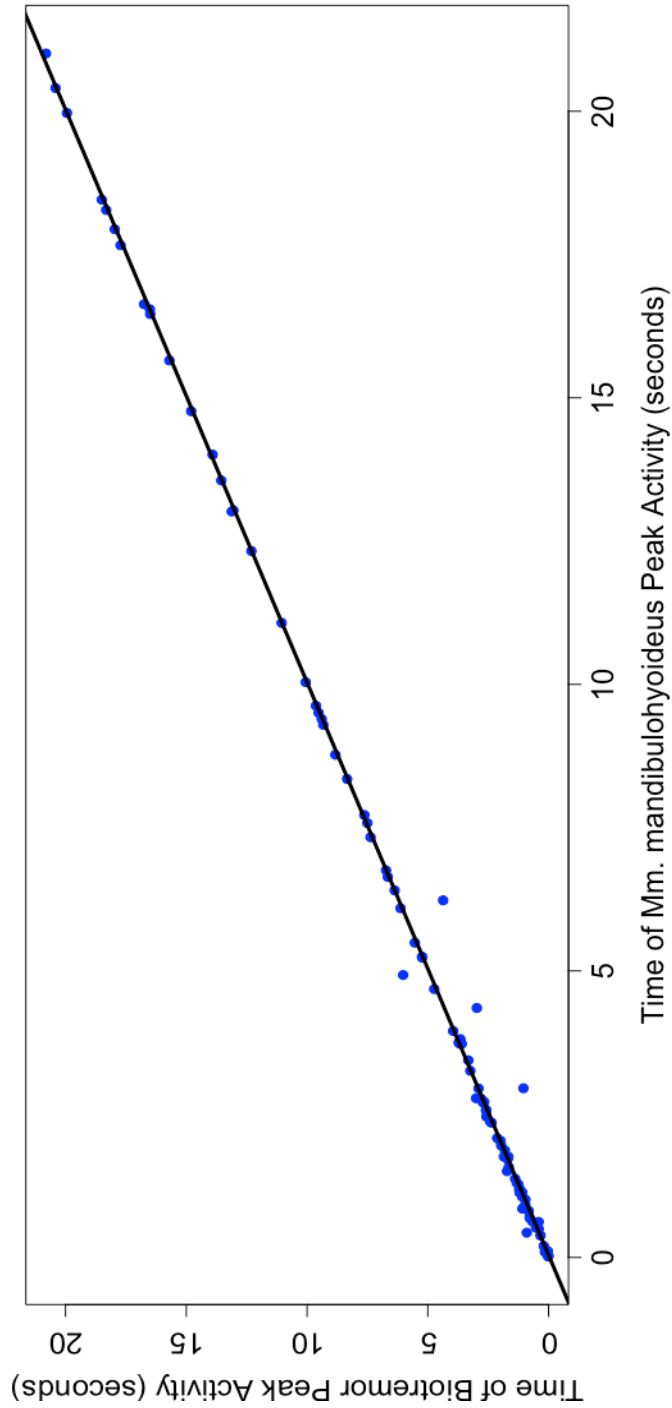


Figure 16: A linear regression of the peak *Mm. levator scapulae* electrical activity and the peak activity of the biotremor. The axes are labeled in seconds, and blue circles indicate the time of a single recorded peak activity of the biotremor and the corresponding time of peak muscular electrical activity. The black line is the line of best fit.

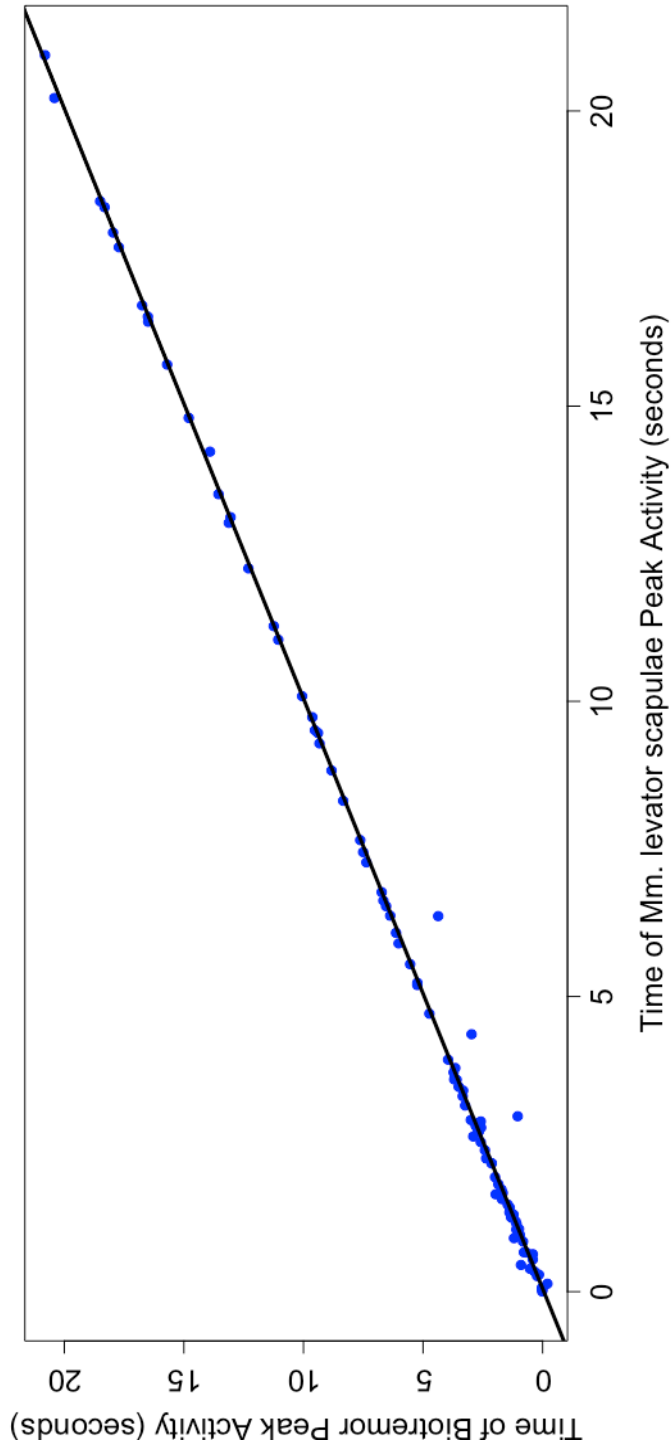


Figure 17: The timing of *M. levator scapulae* (white), *Mm. mandibulohyoideus* (red), *M. sternohyoideus profundus* (yellow), and *M. sternohyoideus superficialis* (orange) activation in relation to the onset, peak activity, and offset of the biotremor. (Photo credit: Marat Nadjibaev)

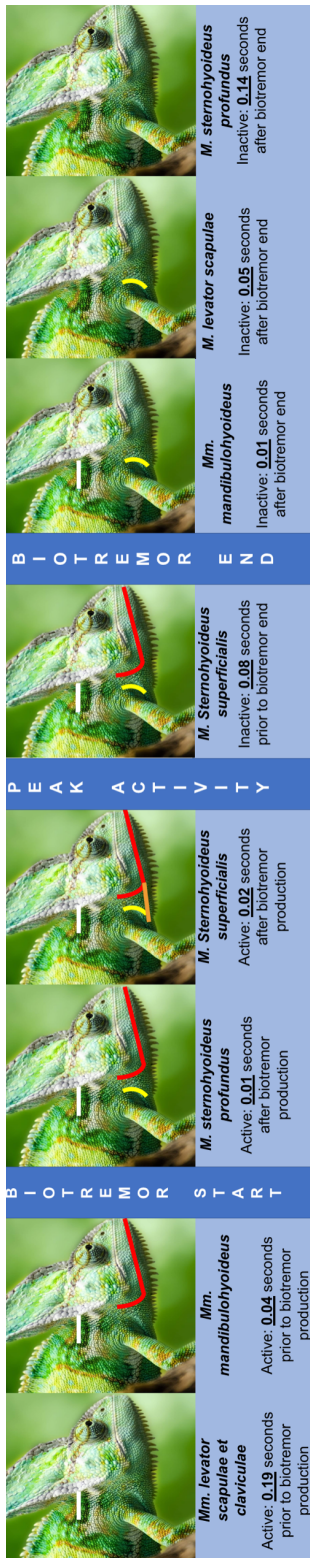


Figure 18: A boxplot of the biotremor frequencies (Hz) for female (yellow) and male (blue) *C. calyptratus*. The colored box indicates first and third quartiles, while the black line in the middle of the box displays the median. The error bars indicate a maximum of 1.5 times the interquartile range for the data, and the large black dots are outside the interquartile range, and small black dots indicate the mean.

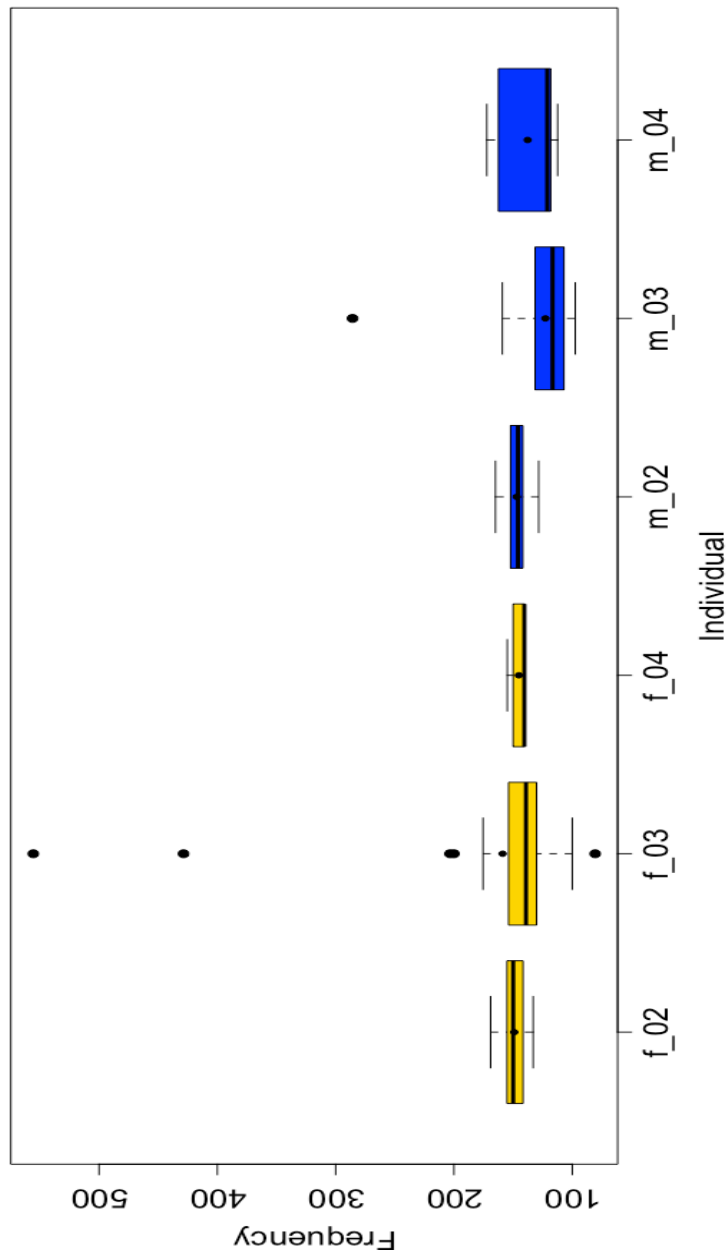


Figure 19: A histogram of the differences in means from empirically generated data sets. The arrow indicates the location of our observed difference in means along the x-axis. The grey bars represent 95% of the distribution and the blue bars represent—the rejection zones—accounting for 5% of the distribution. The black arrow indicates the observed difference in mean frequency between females and males.

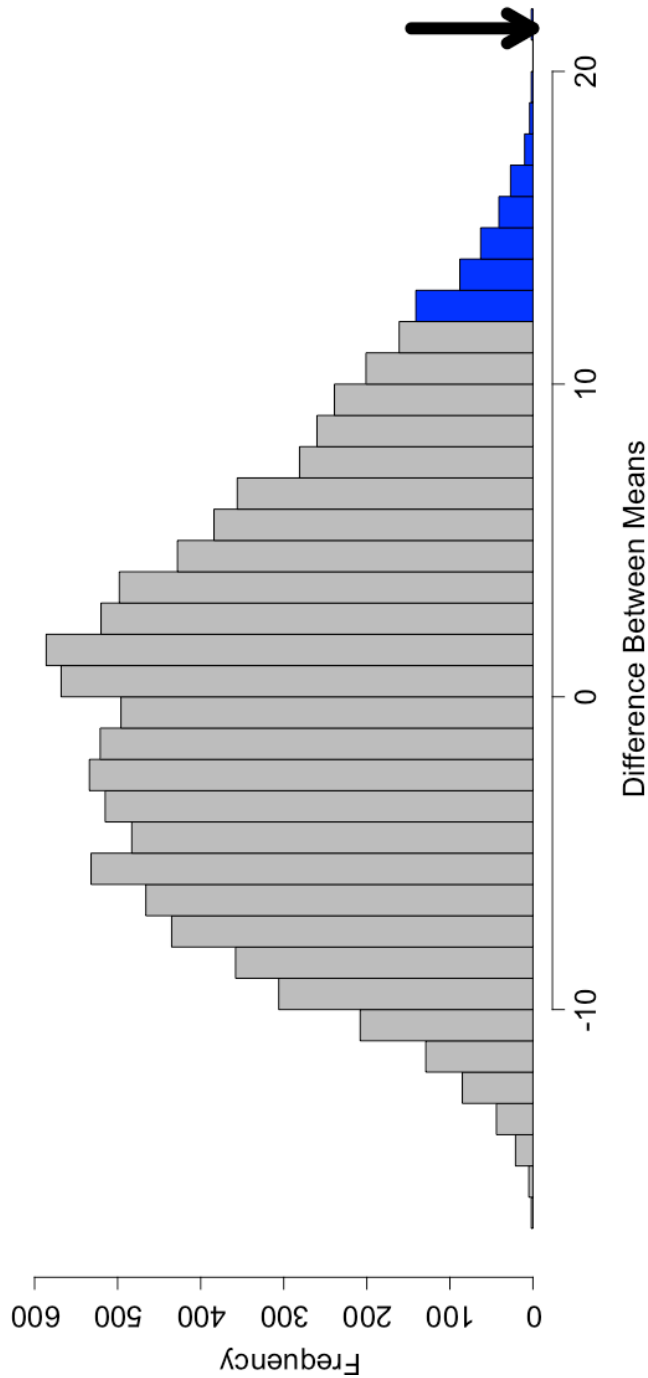


Figure 20: A linear regression of the mean frequencies (Hz) of the biotremors against the size in mass (g) for each individual, indicated by the red and black dots. The sex of each individual is indicated by the color of the dot (red = males and black = females).

